# Longitudinal thermalization via the chromo-Weibel instability

Maximilian Attems

Frankfurt Institute of Advanced Studies

**1207.5795, 1301.7749, 1302.5098**

Collaborators: Anton Rebhan, Michael Strickland

Trento, June 2013

HELMHOLTZ ASSOCIATION

# Motivation

Weakly coupled inspired by Hard Thermal Loops (HTL)

Real-time physical quantities of non-equilibrium processes

Plasma turbulence affects parton transport
(isotropization, jet energy loss, viscosity,..)

Contrast predictions for early time dynamics of the quark gluon plasma

Derivation of time scales for the isotropization, thermalization

# Outline

1. Hard Expanding Loops (HEL)
   - Stages of an heavy ion collision
   - Scales of wQGP
   - Weibel instabilities
   - Yang-Mills Vlasov
   - Bjorken expansion
   - Unstable modes growth rate
2. Physical Observables
   - Numerical tests
   - Energy densities
   - Pressures
   - Spectra
   - Longitudinal temperature

# Assumptions

Free streaming background

Anisotropy in momentum space

SU(2) particle content

Fixed transverse size

Extrapolate to $\alpha_s \sim 0.3$

Match CGC $n(\tau_0) \propto Q_s^3 \alpha_s^{-1}$

# Stages of an heavy ion collision

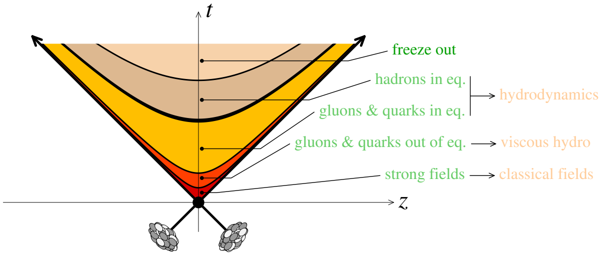


[Gelis 2012] Illustration of the stages of a heavy ion collision.

Numerical approaches to early phase with strong fields:

1. Numerical solution of Yang Mills equations in real-time: [Romatschke, Venugopalan, Berges, Sexty, Gelis, Fukushima, Dusling, Moore, Kurkela, Epelbaum, Schlichting]
2. Hard Loop Simulation (Eikonalized particles): [Strickland, Romatschke, Rebhan, Arnold, Moore, Mrowczynski, Rummukainen, Bödeker, Ipp, Attems, Deja]

# Scales of wQGP

- $T$: energy of hard particles
- $gT$: thermal masses, Debye screening mass,
- $g^2T$: magnetic confinement, color relaxation, rate for small angle scattering
- $g^4T$: rate for large angle scattering, $\eta^{-1}T^4$

# Scales of wQGP

- $T$: energy of hard particles
- $gT$: thermal masses, Debye screening mass, plasma instabilities [Mrowczynski 1988, 1993, ..]
- $g^2 T$: magnetic confinement, color relaxation, rate for small angle scattering
- $g^4 T$: rate for large angle scattering, $\eta^{-1} T^4$

# Weibel instabilities

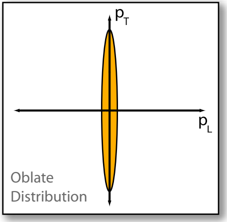


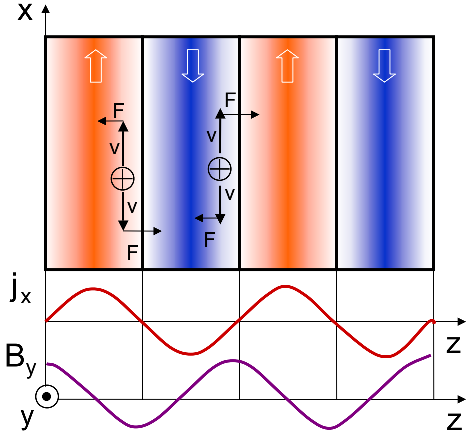


[Mrowczynski 1993,Strickland 2006]: Illustration of the mechanism of filamentation instabilities.

One solves the gauge covariant Vlasov equation

$$V \cdot D \,\delta f^a \Big|_{p^\mu} = g V^\mu F^a_{\mu\nu} \partial^\nu_{(p)} f_0(\mathbf{p}_\perp, p_\eta) \tag{1}$$

# Yang-Mills Vlasov

One solves the gauge covariant Vlasov equation

$$V \cdot D\, \delta f^a \Big|_{p^\mu} = g V^\mu F^a_{\mu\nu} \partial^\nu_{(p)} f_0(\mathbf{p}_\perp, p_\eta) \tag{1}$$

coupled to Yang-Mills equation

$$D_\mu F_a^{\mu\nu} = j_a^\nu = g\, t_R \int \frac{d^3 p}{(2\pi)^3} \frac{p^\mu}{2p^0} \delta f_a(\mathbf{p}, \mathbf{x}, t) \tag{2}$$

One solves the gauge covariant Vlasov equation

$$V \cdot D\, \delta f^a \Big|_{p^\mu} = g V^\mu F^a_{\mu\nu} \partial^\nu_{(p)} f_0(\mathbf{p}_\perp, p_\eta) \qquad (1)$$

coupled to Yang-Mills equation

$$D_\mu F_a^{\mu\nu} = j_a^\nu = g\, t_R \int \frac{d^3 p}{(2\pi)^3} \frac{p^\mu}{2p^0} \delta f_a(\mathbf{p}, \mathbf{x}, t) \qquad (2)$$

in the HTL approximation

$$g A_\mu \ll \left| \mathbf{p}_{hard} \right| . \qquad (3)$$

One solves the gauge covariant Vlasov equation

$$V \cdot D\, \delta f^a \Big|_{p^\mu} = g V^\mu F^a_{\mu\nu} \partial^\nu_{(p)} f_0(\mathbf{p}_\perp, p_\eta) \tag{1}$$

coupled to Yang-Mills equation

$$D_\mu F^{\mu\nu}_a = j^\nu_a = g\, t_R \int \frac{d^3 p}{(2\pi)^3} \frac{p^\mu}{2p^0} \delta f_a(\mathbf{p}, \mathbf{x}, t) \tag{2}$$

in the HTL approximation

$$g A_\mu \ll |\mathbf{p}_{hard}| \,. \tag{3}$$

using the free streaming background distribution function:

$$f_0(\mathbf{p}, x) = f_{\mathrm{iso}}\left(\sqrt{p_\perp^2 + (\frac{p'^z \tau}{\tau_{\mathrm{iso}}})^2}\right) = f_{\mathrm{iso}}\left(\sqrt{p_\perp^2 + p_\eta^2/\tau_{\mathrm{iso}}^2}\right). \tag{4}$$

# Bjorken expansion

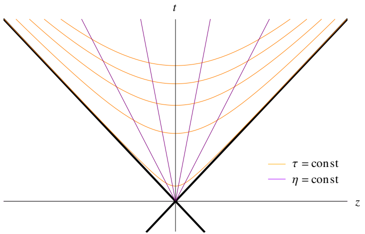

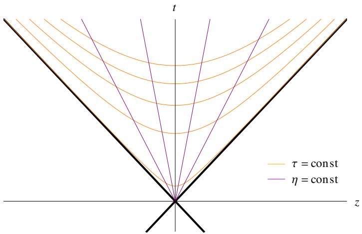


It is convenient to switch to comoving coordinates

$$t = \tau \cosh \eta\,, \qquad \tau = \sqrt{t^2 - z^2}\,,$$
$$z = \tau \sinh \eta\,, \qquad \eta = \mathrm{arctanh}\frac{z}{t}\,, \tag{5}$$

with the corresponding metric

$$ds^2 = d\tau^2 - d\mathbf{x}_\perp^2 - \tau^2 d\eta^2\,. \tag{6}$$

# Unstable modes growth rate

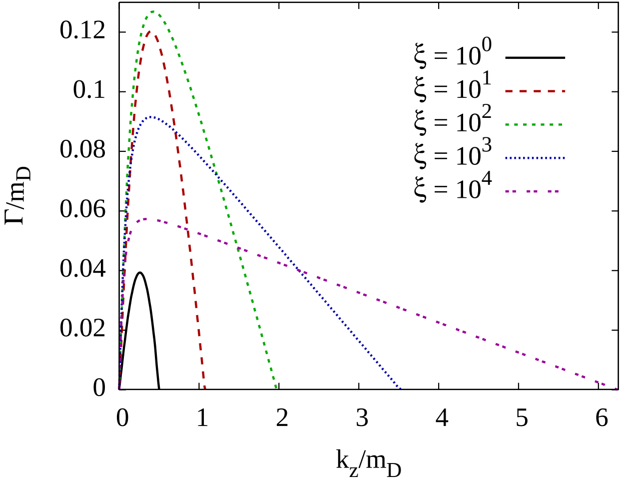


Unstable mode spectra of purely longitudinal modes for specific anisotropies: $N(\tau) \approx \exp(2m_D\sqrt{\tau\tau_{\mathrm{ISO}}})$

# Outline

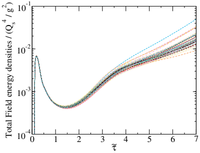


(a) Different seeds

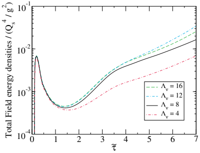


(b) Variation of $\Lambda_\nu$

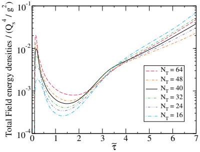


(c) Variation of $a_\perp$

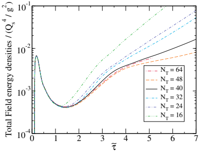


(d) Variation of $N_\perp$

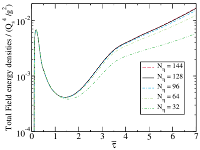


(e) Variation of $a_\eta$

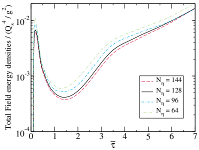


(f) Variation of $N_\eta$

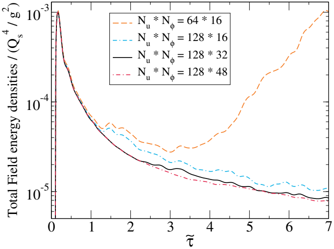


Evolution of stable modes

# Energy densities fields

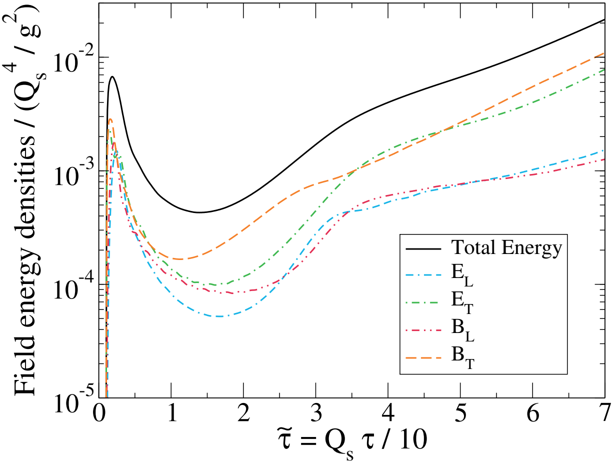


50 averaged runs $N_\perp * N_\eta * N_u * N_\phi = 40^2 * 128 * 128 * 32$:
after onset one sees **rapid growth of $B_l$ and $E_L$ fields**,
followed by non-Abelian interactions kick in.

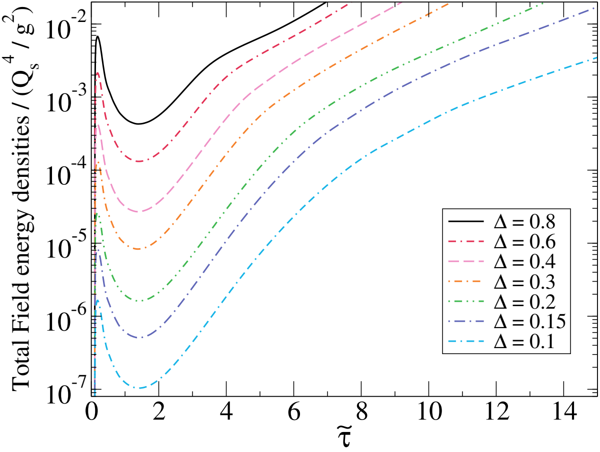


Total field energy density for different initial current fluctuation magnitudes.

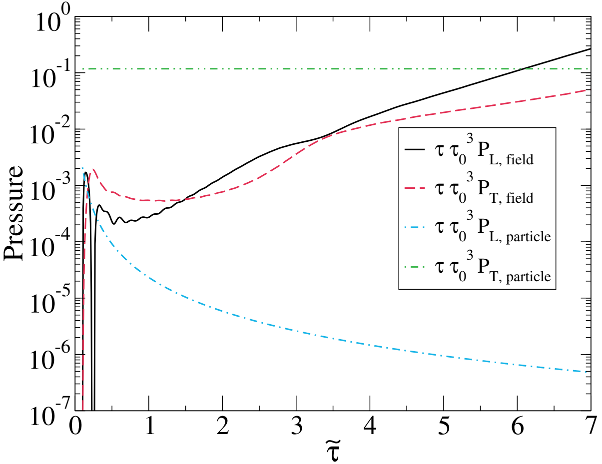


Initially highly anisotropic, note $P_{L,\text{field}}(\tau = 0.3) < 0$, **growing field pressures**, $P_{L,\text{field}}$ dominates at late times, $\tilde{\tau}$ scaled $P_L$ drops $\propto 1/\tilde{\tau}^2$ .

# Pressure ratios

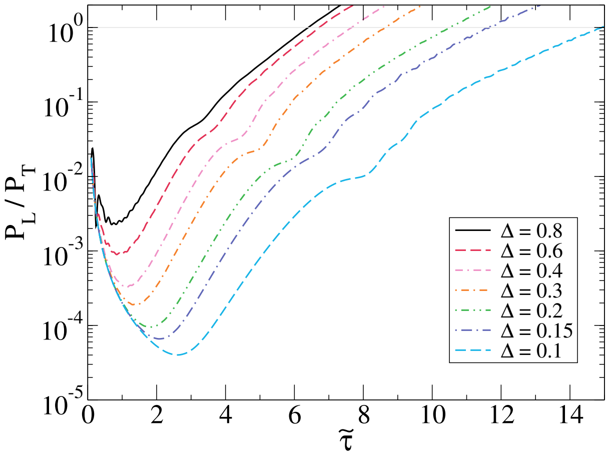


The evolution of the total longitudinal pressure over the total transverse pressure for different initial current fluctuation magnitudes $\Delta$.

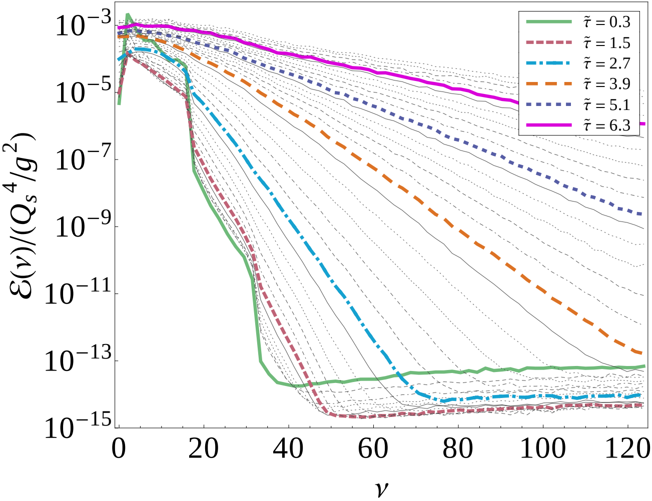


The longitudinal energy spectra at various proper times as a function of $\nu$: **rapid emergence of an exponential distribution of longitudinal energy**.

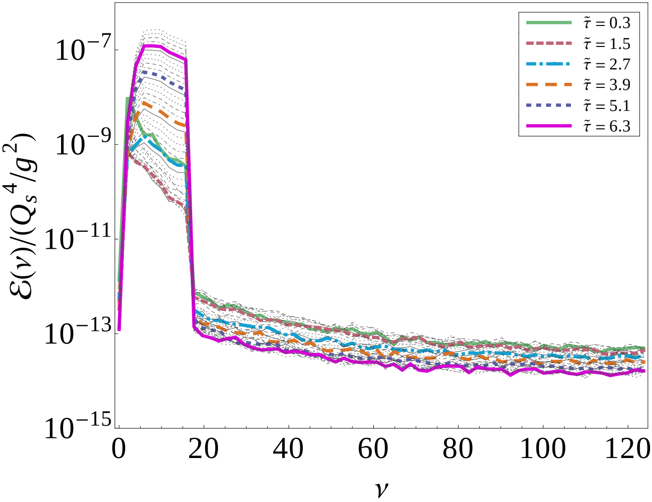


Longitudinal spectra for **abelian** runs shows amplification of the initial seeded modes.

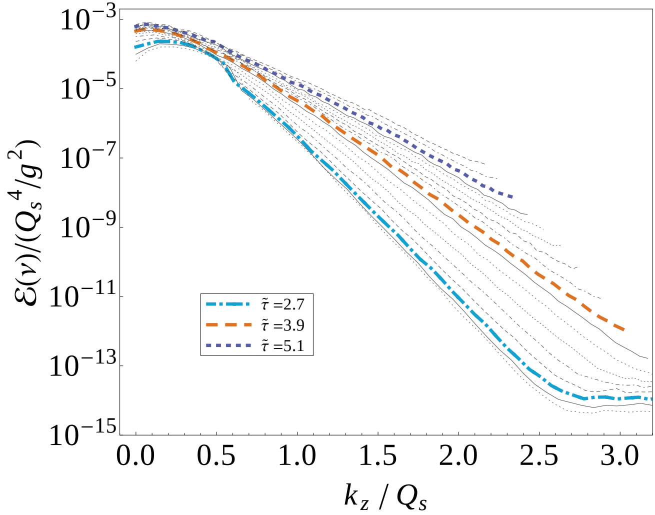


The **red-shifting** is even more visible in the $k_z$ plot. Nonlinear mode-mode coupling is vital in order to populate high momentum modes.

# Spectra

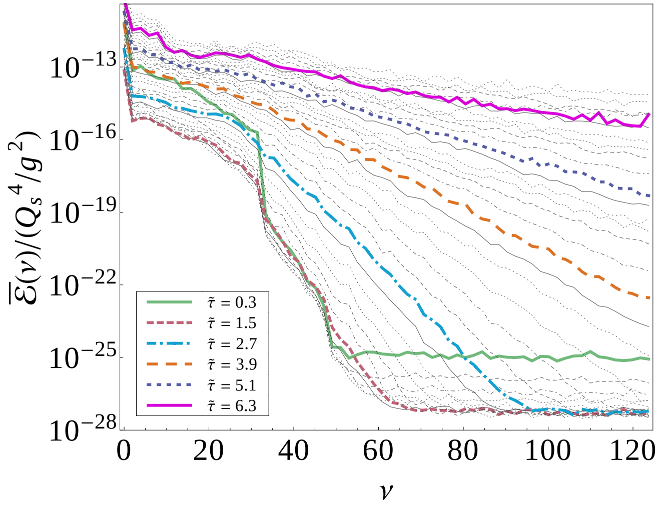

$\overline{\mathcal{E}}(\nu)/(Q_s{}^4/g^2)$
$10^{-13}$
$10^{-16}$
$10^{-19}$
$10^{-22}$
$10^{-25}$
$10^{-28}$
0
20
40
60
80
100
120
$\nu$
$\tilde{\tau} = 0.3$
$\tilde{\tau} = 1.5$
$\tilde{\tau} = 2.7$
$\tilde{\tau} = 3.9$
$\tilde{\tau} = 5.1$
$\tilde{\tau} = 6.3$

Massless Boltzmann distribution fits the longitudinal spectra:

$$\mathcal{E}_{\mathrm{fit}}(k_z) = A\left(k_z^2 + 2|k_z|T + 2T^2\right)\exp\left(-|k_z|/T\right) \qquad (7)$$

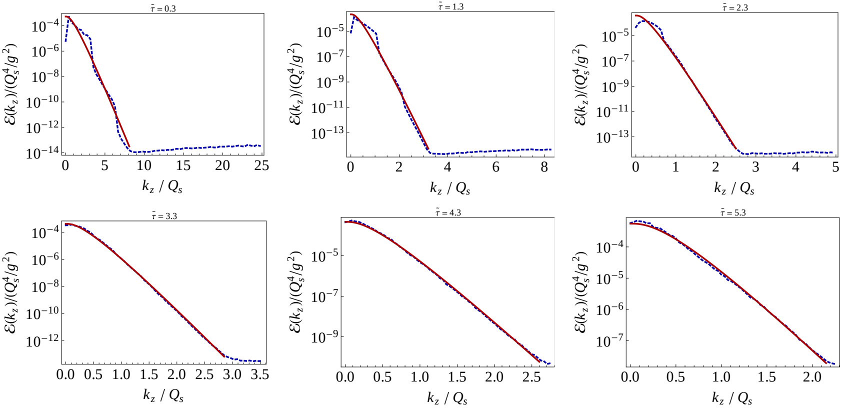


Comparison of data and fit function at six different $\tilde{\tau}$.

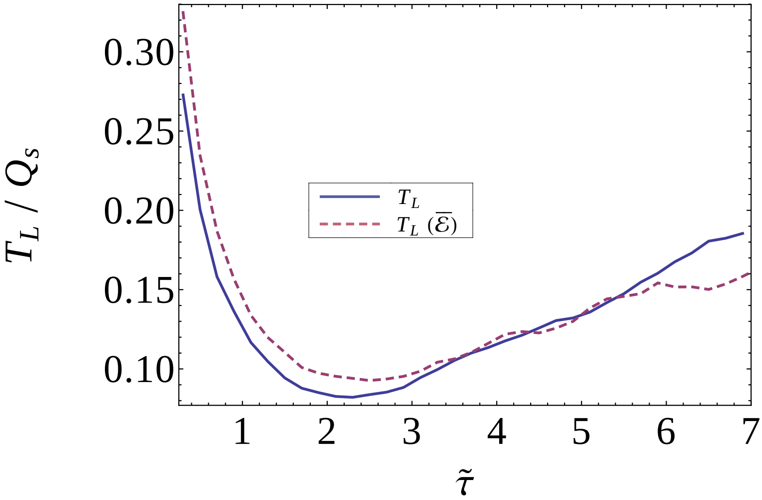


First the soft sector cools down. Due to the instability longitudinal soft **fields reheats**.

# Outlook

- Experimental signatures
- Larger longitudinal $N_\eta$
- Improved IC conditions: $k_\perp$ cutoff
- Measuring the shear viscosity due to plasma instabilities
- Incorporate backreaction
- Pretty visualizations

# Conclusions

- We performed the **first real-time 3d numerical** study of non-Abelian plasma in a longitudinally expanding system within the discretized hard loop framework:
  hard expanding loops HEL.
- The **momentum space anisotropy** can persist for quite some time.
- There doesn't seem to be a "soft scale" saturation of the instability as was seen in static boxes.
- The longitudinal spectra seem to be well described by a Boltzmann distribution indicating **rapid longitudinal thermalization of the gauge fields**.
- Simulations with even larger lattices improving our numerical results are in progress. We are also studying pure Yang-Mills dynamics.

# Backup

Real-time lattice parameters of the evolution in temporal axial gauge:

| | | |
|---|---|---|
| longitudinal lattice spacing | $a_\eta$ | 0.025 |
| transverse lattice spacing | $a$ | $Q_s^{-1}$ |
| temporal time step | $\epsilon$ | $10^{-2}\tau_0$ |
| first time step | $\tau_0$ | $1/Q_s$ |
| longitudinal lattice points | $N_\eta$ | 128 |
| transverse lattice points | $N_\perp$ | $40^2$ |
| lattice size in velocity space | $N_u \times N_\phi$ | $128 \times 32$ |
| coupling constant | $g$ | $(3.77)^{0.5}$ |

Assuming for LHC collisions

$$Q_s \sim 2\mathrm{GeV} = (0.1\mathrm{fm})^{-1}\ . \tag{8}$$

We match to CGC values

$$n(\tau_0) = c\,\frac{N_g Q_s^3}{4\pi^2 N_c \alpha_s (Q_s \tau_0)} \tag{9}$$

with the gluon liberation factor $c = 2\ln 2$. From this one can determine the isotropic Debye mass

$$m_D^2(\tau_{\mathrm{ISO}}) = 1.285/(\tau_0 \tau_{\mathrm{ISO}}). \tag{10}$$